

Peripheral Ossifying Fibroma and Juxtacortical Chondrosarcoma in Cynomolgus Monkeys (*Macaca fascicularis*)

Barthel Schmelting,^{1,*} Martina Zöller,^{2,†} and Joachim Kaspareit²

Literature on spontaneous primary bone tumors in nonhuman primates is sparse. This case report describes 2 different neoplastic bone lesions in 2 adult cynomolgus monkeys (*Macaca fascicularis*), including macroscopic, radiographic, histologic, and immunohistochemical findings. In one monkey, a firm mass located at the palatogingival junction of the left rostral maxilla was confirmed to be a peripheral ossifying fibroma in light of its histologic and immunohistochemical characteristics. In another monkey, a lobulated tumor at the right distal femur that radiographically showed moderate radiopacity with splotchy areas of mineralization was confirmed to be a juxtacortical chondrosarcoma on histologic examination. The 2 neoplastic bone lesions revealed rare histologic and immunohistochemical characteristics and contribute to the known tumor spectrum of cynomolgus monkeys.

Spontaneous primary bone tumors are rare in nonhuman primates.²³ Only few references can be found on osteomas, osteosarcomas, and osteogenic sarcomas in various nonhuman primate species, including rhesus macaques (*Macaca mulatta*),¹ squirrel monkeys (*Saimiri sciureus*),^{15,26} stump-tail monkeys (*Macaca arctoides*),⁴ Japanese monkeys (*Macaca fuscata*),³⁴ and baboons (*Papio* spp.).^{5,28} In addition, a giant cell tumor of the ulna in a chacma baboon (*Papio porcarius*) has been reported.²⁵ Descriptions of cartilaginous bone tumors in nonhuman primates are limited to a chondrosarcoma of the nasal bone in a squirrel monkey (*Saimiri sciureus*)³ and a fibrochondroma of the larynx in a tamarin monkey.⁶ Reports on spontaneous bone tumors in cynomolgus monkeys (*Macaca fascicularis*) are nonexistent, according to our literature search. At our facility, a total of 33 tumors were observed in cynomolgus monkeys during a 15-y time period; none of these tumors was identified as a bone tumor.¹⁴

In the present case report, we describe the radiographic, macroscopic, histologic, and immunohistochemical features of 2 rare bone tumors, a peripheral ossifying fibroma of the maxilla and a juxtacortical chondrosarcoma of the femur. These tumors occurred in 2 adult cynomolgus monkeys.

Case Reports

Animals and husbandry. Both animals were purpose-bred male adult cynomolgus monkeys that belonged to the stock colony of the facility. These monkeys were single-sex pair-housed in a climate-controlled room with a minimum of 10 air changes hourly. The temperature and relative humidity ranges were 19 to 25 °C and 40% to 70%, respectively. Artificial lighting was controlled automatically to give a 12:12-h light:dark cycle. Each cage (height, 248 cm; width, 151.5 cm; depth, 151 cm) was provided

with objects for environmental enrichment, including movable stainless steel mirrors, colored plastic tools, and colored plastic balls. The bottom of the cages was enriched with wooden chips. A specialized primate diet (Sniff Pri 10 mm; sSniff Spezialdiäten GmbH, Soest, Germany) was offered twice daily. The monkeys regularly received fresh fruit and bread as food supplements. Tap water was provided ad libitum through an automatic watering system. Housing and handling of the monkeys were in compliance with applicable federal regulations governing the use of animals in research and with AAALAC guidelines. All uses and procedures were approved and in accordance with the Institutional Animal Care and Use Committee of Covance Laboratories GmbH.

Radiographic examinations were performed under general anesthesia with ketamine hydrochloride (10 mg/kg body weight IM; Ketavet, Pharmacia GmbH, Berlin, Germany) by using a digital imaging system (DX-S, Agfa-Gevaert, Mortsel, Belgium). Euthanasia was performed by ketamine anesthesia followed by intravenous overdose of sodium pentobarbital (400 mg/kg body weight; Release, WdT, Garbsen, Germany).

Case 1. A 7-y-old male cynomolgus monkey of Mauritian origin (weight, 7.7 kg; free of B virus, measles virus, simian retrovirus, simian T-cell leukemia virus, *Mycobacterium* spp., *Salmonella* spp., *Shigella* spp., and *Yersinia* spp.) presented clinically with a slow-growing, round to oval, broad-based, firm mass of 2 × 2 × 1.5 cm at the palatogingival junction of the left rostral maxilla. The mass partially penetrated the interdental spaces between the left incisors and left canine, leading to lateral displacement of the left second incisor (I2). However, food intake was not impaired. The overlying gingival mucosa was pinkish to light red and nearly intact, with the exception of a few pinpoint-sized erosions (Figure 1). Radiographic examination revealed a faint radiolucent lesion with multifocal central spots of increased radiopacity (mineralized foci) superimposed on the underlying normal bone architecture of the maxilla. Other than displacement of the left incisor and canine, there were no obvious radiographic alterations of the teeth (Figure 2). Because

Received: 14 Apr 2010. Revision requested: 04 May 2010. Accepted: 28 May 2010.
Departments of ¹Veterinary Services and Colony Management and ²Pathology, Covance Laboratories GmbH, Muenster, Germany.

[†]Current affiliation: Pathology Unit, German Primate Center, Goettingen, Germany.

*Corresponding author. Email: barthel.schmelting@covance.com



Figure 1. Oral mass in the maxilla in a 7-y-old cynomolgus monkey.



Figure 2. Radiographically, the mass presented as an expansile, radiolucent lesion (arrows) with multiple foci of faint mineralization (laterolateral view).

the mass could not be excised surgically, the monkey was euthanized and submitted for necropsy.

Case 2. A 4-y-old male cynomolgus monkey of Mauritian origin (weight, 6.6 kg; free of B virus, measles virus, simian retrovirus, simian T-cell leukemia virus, *Mycobacterium* spp., *Salmonella* spp., *Shigella* spp., and *Yersinia* spp.) showed a progressively growing, round, firm mass measuring approximately 6 × 6 × 7 cm attached to the medial side of the right distal femur (Figure 3). Radiographically, there was a large soft tissue mass of moderate radiopacity and splotchy areas of mineralization. In the underlying bone, slight erosions and an irregular sclerotic reaction in the cortex of the epimetaphysis and distal part of the diaphysis of the femur were apparent. Cortical thickening was noted at the proximal margin of the lesion (Figure 4).

Pathologic examinations

Complete necropsies were performed on both animals. Samples from numerous diverse organs as well as the maxilla and right femur were fixed in 10% neutral buffered formalin for approximately 2 d. The maxilla and the right femur were decalcified in Kristenson fluid for at least 2 wk to allow slicing of the bony structures. Tissue samples were processed routinely, embedded in paraffin, sectioned at 5 μm, and stained with hematoxylin and eosin. Immunohistochemistry was performed on paraffin-embedded sections of the oral and femoral masses



Figure 3. Mass at the right medial distal thigh in a 4-y-old cynomolgus monkey.

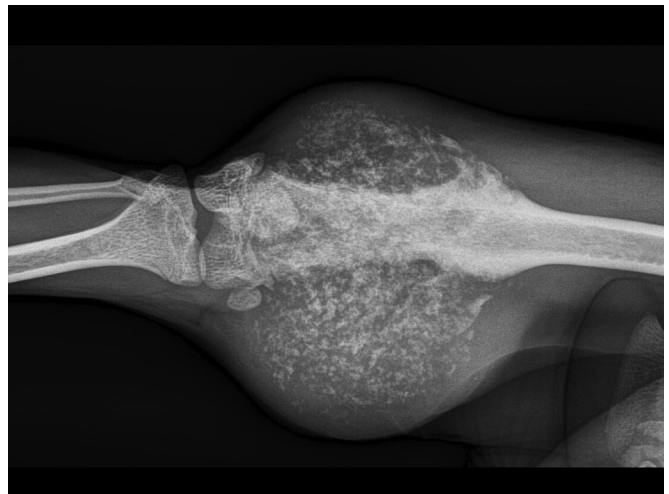


Figure 4. Radiography of the femoral mass revealed a large mass with moderate radiopacity and multifocal floccular mineralization. The underlying bone is characterized by diffuse cortical lysis, patchy remodeling processes involving the medullary cavity, and cortical thickening at the proximal margin of the lesion. There is obvious soft tissue extension.

by using various primary antibodies (Figure 5). Antibody diluent with background reducing components (DakoCytomation GmbH, Hamburg, Germany) served as a negative control for all primary antibodies. The slides were counterstained with Mayer hemalaun (Merck, Darmstadt, Germany). Microscopic evaluation of the immunohistochemical results included the estimated percentage (%) of immunoreactive neoplastic cells and antigen localization (nuclear, cytoplasmic, or both).

Case 1. Macroscopically, the solid tumor in the maxilla of animal number 1 had a white homogeneous cut surface with multiple foci of mineralization and showed distinct demarcation from the underlying bony tissue. No other macroscopic findings were observed at necropsy. Histologic examination revealed a poorly to moderately cellular, expansile, well-demarcated, un-

Antigen	Commercial name	Dilution	Pretreatment	Method of staining	Positive control
Desmin	Monoclonal mouse antihuman desmin, clone D33	1:75	Target retrieval solution (pH 9.0)	Alkaline-phosphatase–antialkaline-phosphatase technique with fuchsin as the chromogen	Tongue
Ki67	Monoclonal mouse antihuman Ki67, clone MIB1	1:150	Citrate buffer (pH 6.0)	Peroxidase–antiperoxidase technique with diaminobenzidine as the chromogen	Small intestine
Pancytokeratin	Monoclonal mouse antihuman cytokeratin, clone LP34	1:100	Tris–EDTA buffer (pH 9.0)	Peroxidase–antiperoxidase technique with diaminobenzidine as the chromogen	Skin
S100	Polyclonal rabbit antiS100	1:1000	Protease	Streptavidin–biotin technique with diaminobenzidine as the chromogen	Brain
Smooth-muscle actin	Monoclonal mouse antihuman smooth-muscle actin, clone 1A4	1:50	Citrate buffer (pH 6.0)	Labeled streptavidin–biotin technique with diaminobenzidine as the chromogen	Uterine wall
Vimentin	Monoclonal mouse antihuman vimentin, clone V9	1:75	Target retrieval solution (pH 9.0)	Alkaline-phosphatase–antialkaline-phosphatase technique with fuchsin as the chromogen	Skin

Figure 5. Details of the primary antibodies (all obtained from DakoCytomation, Hamburg, Germany) and staining methods for the immunohistochemical characterization of both tumor masses. All positive-control tissues were from *M. fascicularis*.

encapsulated neoplasm expanding the submucosal connective tissue of the gingiva. The tumor was composed of a collagen-rich spindle cell proliferation multifocally interspersed with trabecular bone (Figure 6). Neoplastic fibroblastoid cells had indistinct cell borders; a faintly eosinophilic, fibrillar cytoplasm; and elongated nuclei. Mitotic figures were not apparent. However, immunohistochemical examination revealed nuclear Ki67 expression in single fusiform cells. Neoplastic cells also showed weak, diffuse nuclear and cytoplasmic expression of S100 and distinct diffuse cytoplasmic expression of smooth-muscle actin and vimentin (Figure 7) but were negative for pancytokeratin and desmin (Figure 8). The islands of mineralized bony matrix were lined partially by osteoblasts and a few osteoclasts and sporadically contained osteocyte lacunae. Multifocally, areas of dystrophic calcification and small deposits of cementum-like material (forming basophilic tide lines) were present within the osseous trabeculae. At the transition to the underlying maxillary bone, there were multifocal areas of bone resorption. The lingual surface of the left second incisor had intact gingival attachment, but the alveolar crest and periodontal ligament were partially replaced by fibrous proliferative tissue that extended to the dental surface. Several small foci of lymphohistiocytic inflammatory cell infiltrates were present throughout the tumor mass. All other organs were histologically unremarkable.

On the basis of the tumor location and the histologic and immunohistochemical characteristics, the maxillary mass was classified as a peripheral ossifying fibroma.

Case 2. At necropsy, the mass originating from the femoral surface appeared as a gray-white, homogenous, partly lobulated cut surface with infiltrative growth into the adjacent femoral bone and skeletal muscles. However, there was no obvious involvement of the articular surfaces of the knee joint. The tumor was strongly mineralized and was hardly sliceable prior to decalcification. Capsular demarcation was absent. Histologically, there was a moderately to highly cellular, infiltrative, not demar-

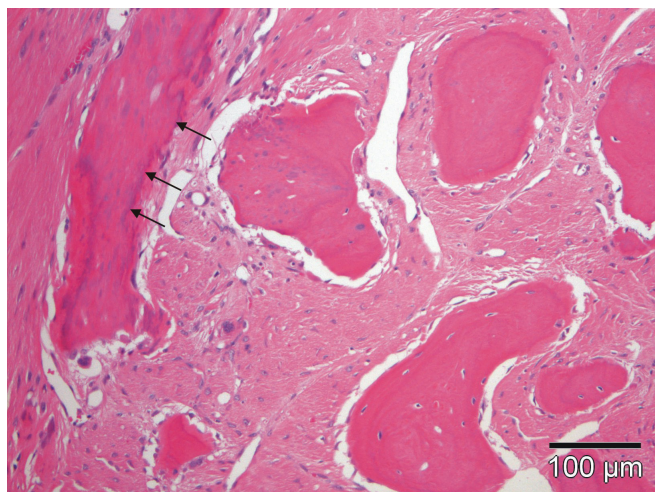


Figure 6. The maxillary tumor was composed of fibrous connective tissue with neoplastic fibroblastoid cells and bony islands that were characterized by deposits of dystrophic calcification and cementum-like material (arrows). The bone trabeculae were lined by osteoblasts and individual osteoclasts and contained osteocyte lacunae. Hematoxylin and eosin stain; scale bar, 100 μ m.

cated, unencapsulated mass originating from the distal femoral cortex. The tumor was composed of irregular cartilaginous lobules separated by thin fibrovascular stroma bands. The lobules generally consisted of a poorly cellular cartilaginous matrix core of variable differentiation surrounded by a densely cellular rim, with small, undifferentiated, oval to polygonal mesenchymal cells in the lobule periphery (Figure 9). The undifferentiated small cells had oval to elongated nuclei with 1 to 2 nucleoli, indistinct cell borders, and contained moderate amounts of eosinophilic, partly granular or vacuolated cytoplasm. Central parts of the lobules revealed abundant amorphous basophilic chondroid matrix, multifocally undergoing hyalinization, dys-

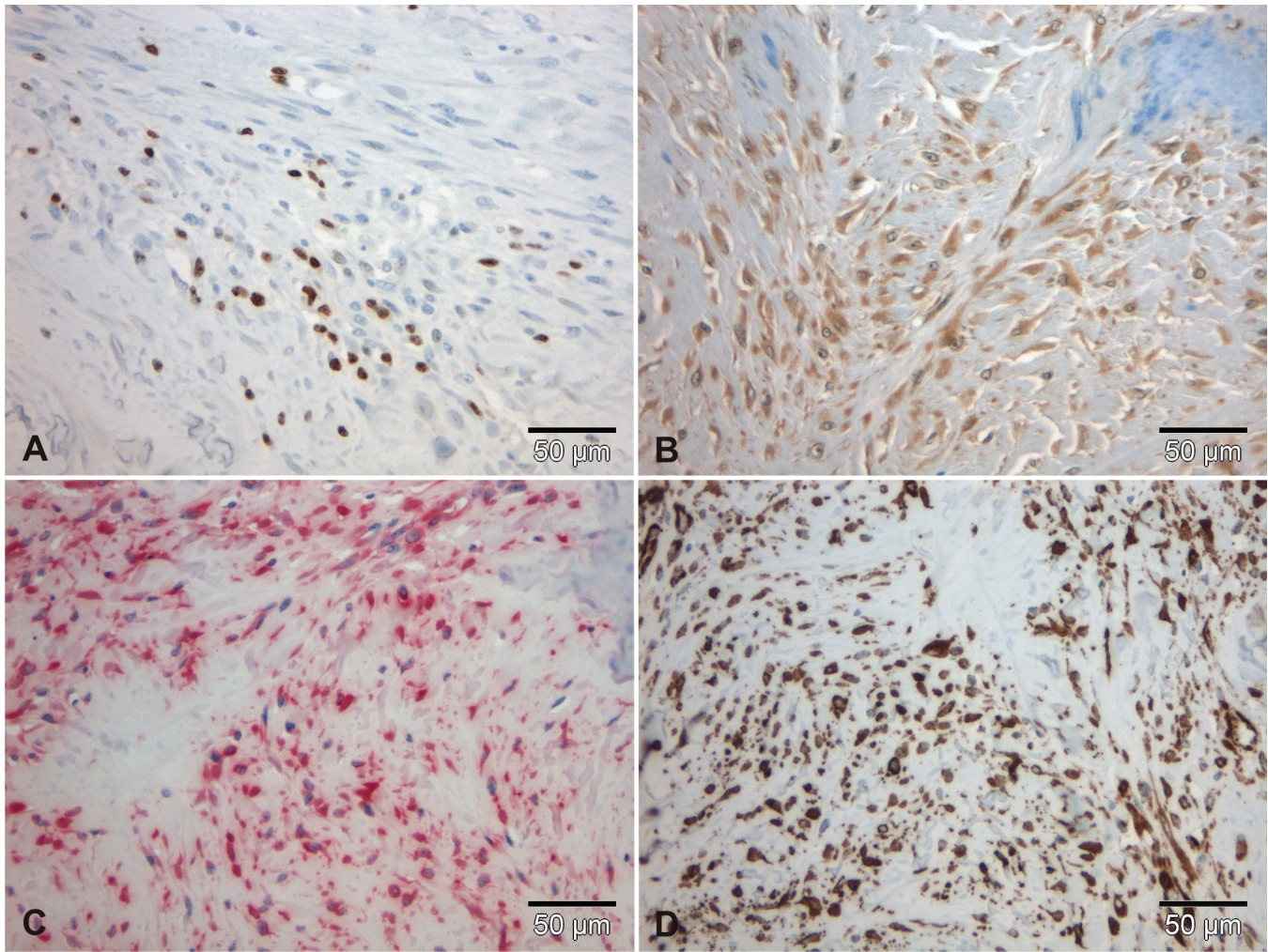


Figure 7. Immunohistochemical staining profile of the tumor in case 1. (A) A few cells showed nuclear expression of Ki67. (B) Almost all neoplastic cells showed weak immunoreactivity for S100. All spindle cells revealed nuclear and cytoplasmic expression of (C) vimentin and (D) smooth-muscle actin. Scale bar, 50 µm.

Antigen	Ossifying fibroma (case 1)	Chondrosarcoma (case 2)
Desmin	negative	1%, cytoplasmic
Ki67	5%, nuclear	70%, nuclear
Pancytokeratin	negative	negative
S100	90%, nuclear and cytoplasmic	100%, nuclear and cytoplasmic
Smooth-muscle actin	100%, cytoplasmic	100%, cytoplasmic
Vimentin	100%, cytoplasmic	100%, cytoplasmic

Figure 8. Immunohistochemical staining results indicating the approximate percentage of immunoreactive cells and antigen localization in both tumors.

trophic calcification, or enchondral ossification. In these areas, the variably sized, polygonal neoplastic cells were characterized by distinct anisocytosis and anisokaryosis. Multiple binucleated cells were present. Mitotic activity was variable, ranging from less than 1 to 10 mitotic figures per high-power field and correlated with the Ki67 expression pattern of the tumor. Cytoplasmic expression of vimentin and smooth-muscle actin was present in both mature and undifferentiated neoplastic cells. Tumor cells further showed nuclear and cytoplasmic S100 ex-

pression of varying intensity (Figure 10). Individual cells were also positive for desmin (cytoplasmic staining). Immunoreactivity for pancytokeratin was absent (Figure 8). Large areas of necrosis were present throughout the tumor mass. The lesion showed infiltrative growth into the adjacent skeletal muscles and invaded cortical and medullary parts of the underlying femoral bone, leading to multifocal osteolysis of preexisting bone. There was no evidence of metastasis in regional lymph nodes or other organs.

Given its macroscopic, histologic, and immunohistochemical characteristics, the femoral tumor was diagnosed as a juxtacortical chondrosarcoma.

Discussion

Ossifying fibromas (also known as cemento-ossifying fibromas) are benign, solitary, progressively expansile, fibroosseous neoplastic lesions primarily affecting the jaws and leading to distortion of normal bone contour, displacement and loss of teeth, and difficulties in food uptake.^{7,32} They have been reported to occur in the maxilla or mandible of humans^{7,33,35} and various animals, including horses,^{20,30} greater kudu,² llamas,¹⁸ rabbits,³² sheep,^{27,30} dogs,^{17,19,30} and cats.^{30,31} These tumors are believed to arise from cells of the periodontal ligament or periosteum and can be subdivided into peripheral ossifying

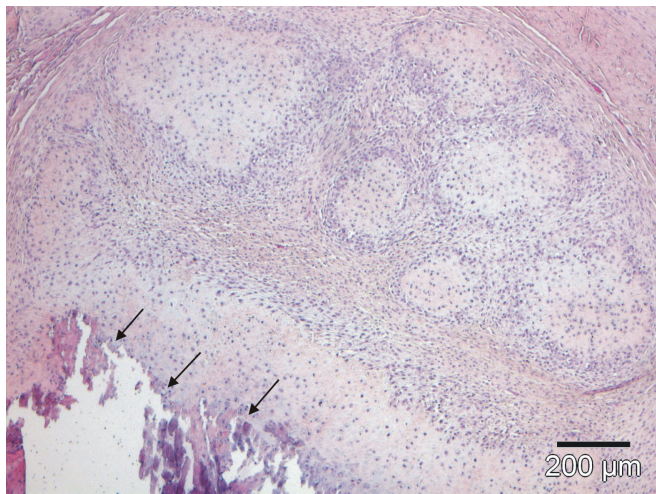


Figure 9. The femoral tumor was composed of lobules with a poorly cellular cartilaginous matrix core surrounded by a densely cellular rim of undifferentiated polygonal mesenchymal cells. Multifocally, central lobule parts underwent dystrophic calcification (arrows). Hematoxylin and eosin stain; scale bar, 200 μm .

fibromas, which have a superficial, gingiva-associated localization, and central ossifying fibromas, which are located within the jaw bones.^{7,16} Radiographically, well-demarcated mixed or moderately radiolucent lesions can be seen in the maxilla or mandible, especially in the tooth-bearing anterior region.⁸ Histologically, ossifying fibromas are characterized by fibrous connective tissue containing variable amounts of fibroblasts, myofibroblasts, and collagen and by the presence of mineralized material, which may represent mature, lamellar, or woven osteoid; cementum-like material; or dystrophic calcifications.^{16,30} Islands of bone are often surrounded by active osteoblasts (that is, osteoblastic rimming). In addition, acute or chronic inflammatory cells can be identified in the lesion.^{16,30}

The histopathologic features of the neoplasm in case 1 are consistent with those described for peripheral ossifying fibromas. The clear demarcation from the underlying bony tissue and presence of osteoblasts surrounding the bony spicules helped to differentiate this lesion from the condition of fibrous dysplasia, which generally lacks osteoblastic rimming and the characteristic sharp demarcation between lesional and normal bone.^{18,32} The immunohistochemical staining pattern confirmed the myofibroblastic nature of the neoplastic spindle cells, because they expressed both vimentin and smooth-muscle actin. Interestingly, many neoplastic cells also expressed S100 protein, which draws into question an exclusively myofibroblastic origin. However, S100 expression was reported to occur in a human case of a cemento-ossifying fibroma of the craniofacial skeleton⁹ and is described (also called osteofibrous dysplasia) to occur in more than 50% of ossifying fibromas of the tibia or fibula in children.²⁹ The significance of the S100 expression in the tumor of the cynomolgus monkey we present here is unclear and gives reason for reconsideration of the tumor cell histogenesis of gnathic ossifying fibromas.

Regarding the occurrence of ossifying fibromas in nonhuman primates, a comparable lesion with a similar microscopic appearance with the diagnosis of bilateral fibroosteoma in the left and right maxilla of a young female rhesus monkey (*Macaca mulatta*) has been described.²⁴ However, due to the bilateral symmetric tumor formation and their histologic resemblance

to disorders of calcium metabolism and ossification, the author could not completely rule out a generalized condition of fibrous osteodystrophy.

Ossifying fibromas generally show a benign biologic behavior. Malignant transformation has not been reported for this lesion, but the recurrence rate after surgical removal may be as high as 20%. Treatment consists of local surgical excision including the periodontal ligament and the periosteum.^{7,16,30} In the case of the cynomolgus monkey case presented here, euthanasia was elected as success of preservative surgical excision was doubtful.

Chondrosarcomas are malignant mesenchymal tumors, in which the neoplastic cells produce variable quantities of cartilaginous matrix.³⁰ They are the third most common primary malignant tumor of bone in humans and usually develop in the trunk, pelvis, and long bones of middle-aged patients.¹¹ In domestic animals, the dog is the most commonly affected species (10% of primary bone tumors). In other domestic and laboratory animal species, spontaneous chondrosarcomas of bone are relatively rare.^{10,30} The only reported case of chondrosarcoma in nonhuman primates is that of a lesion of the nasal bone in a squirrel monkey (*Saimiri sciureus*).³ In humans, several subtypes (incorporating both location and histologic characteristics) of primary chondrosarcomas have been described, including conventional intramedullary, clear cell, myxoid, mesenchymal, dedifferentiated, extraskeletal, and juxtacortical forms.^{21,22} The juxtacortical forms represent a rare manifestation of chondrosarcomas in humans (fewer than 2% of all chondrosarcomas) and applies to the presented case in a cynomolgus monkey. Radiographs of juxtacortical chondrosarcomas typically demonstrate round to oval radiolucent masses on the surface of bone, mainly on the distal femur, with chondroid matrix mineralization, often described to be 'popcornlike,' and cortical thickening.¹² Macroscopically, the cut surfaces of chondrosarcomas typically have a lobulated architecture with alternating translucent (hyaline cartilage) and white granular areas (mineralization). Although results from clinical and macroscopic examinations and imaging techniques generally give first evidence for the presence of juxtacortical chondrosarcomas, the main differential diagnoses of periosteal osteosarcoma and periosteal chondroma often can only be excluded by histologic examination, which reveals lobules of hyaline cartilage with areas of matrix mineralization and enchondral ossification as well as entrapment and destruction of trabecular bone. Osteoid is lacking.^{21,22} In general, juxtacortical can rarely involve the medullary cavity.¹² However, the tumor of case 2 focally showed medullary invasion, which did not become apparent from the radiographic pictures due to the lack of mineralization of the neoplastic lesion in this location.

In the presented case, immunohistochemical staining with anti-S100 antibody confirmed the chondrocyte histogenesis of the neoplastic cells, whereas the intensity of the nuclear and cytoplasmic staining depended on the degree of cellular differentiation. Mature, intensely stained chondrocytes generally were located in the centers of the cartilaginous lobules that were surrounded by less differentiated, weakly stained neoplastic cells at the lobule periphery. Vimentin expression confirmed the mesenchymal origin of the tumor. The chondrosarcoma of the cynomolgus monkey also expressed desmin and smooth-muscle actin. Expression of these cytoskeletal proteins, which is indicative of smooth muscle differentiation, has been reported occasionally for chondrosarcomas in humans, especially for mesenchymal subtypes that represent primitive neoplasms with polyphenotypic differentiation.^{11,13} The immunohistochemical profile of the juxtacortical chondrosarcoma of our cynomolgus

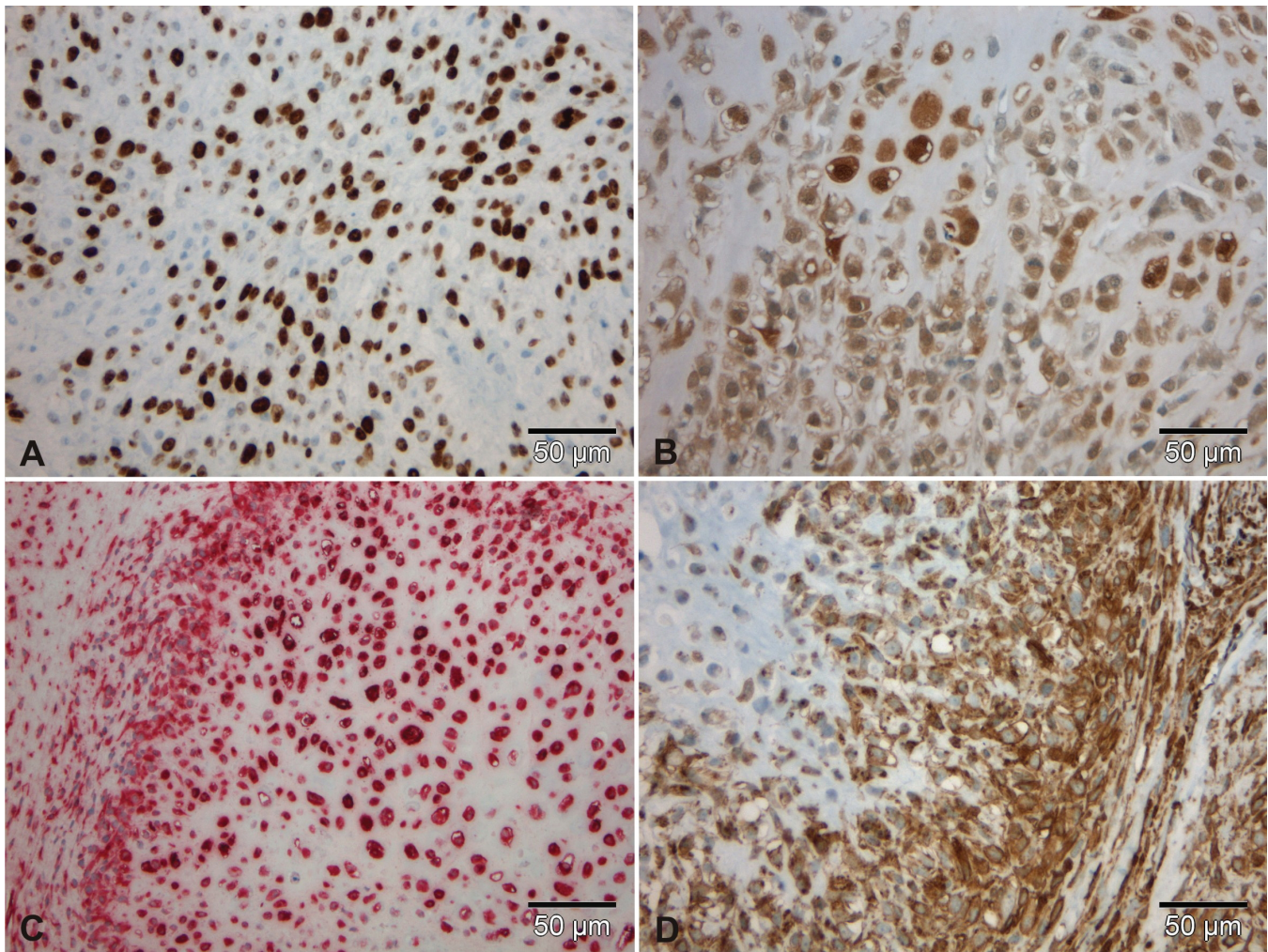


Figure 10. Immunohistochemical staining profile of the tumor in case 2. (A) Many cells show nuclear expression of Ki67. (B) All neoplastic cells show nuclear and cytoplasmic immunoreactivity for S100 as well as nuclear and cytoplasmic expression of (C) vimentin and (D) smooth-muscle actin. Scale bar, 50 µm.

monkey therefore suggests a rather poorly differentiated tumor, a diagnosis also supported by its cellular histomorphology, mitotic rate (correlating with nuclear Ki67 expression in the neoplastic cells), and extensive necrotic areas.

Compared with conventional medullary chondrosarcomas, juxtacortical chondrosarcomas are less aggressive in terms of invasive growth and metastasis. Even with less-differentiated tumors, the prevalence of metastasis and local recurrence after surgical excision is low.²¹ In the present case, there was no evidence of metastasis. However, euthanasia of the monkey was indicated, given that surgery would have involved amputation of the femur, and reconstructive measures were regarded to be impractical in terms of the monkey's use in toxicologic studies.

In conclusion, 2 different rare neoplastic bone lesions—a peripheral ossifying fibroma of the maxilla and a juxtacortical chondrosarcoma of the femur—with rare histologic and immunohistochemical characteristics occurred in 2 adult cynomolgus monkeys. Because cynomolgus monkeys are commonly used laboratory animals in toxicologic studies, comprehensive knowledge about naturally occurring neoplastic disease is essential for the characterization of spontaneous pathology of this animal species. Therefore, the case descriptions presented here contribute to the known tumor spectrum in cynomolgus monkeys.

Acknowledgments

We thank the Veterinary Services technical assistants as well as the necropsy and histology team of Covance Laboratories GmbH (Münster, Germany) for their excellent technical assistance and laboratory work and Nadine Knöchelmann for performing the S100 immunohistochemistry.

References

1. Beam SL. 2005. Combined-type osteosarcoma in a rhesus macaque. *Vet Pathol* 42:374–377.
2. Boever WJ, Kennedy S, Kane KK. 1977. Ossifying fibroma in a greater kudu. *Vet Med Small Anim Clin* 72:1483–1486.
3. Chalifoux LV. 1993. Chondrosarcoma, squirrel monkey, p 128–131. In: Jones TC, Mohr U, Hunt RD, editors. *Nonhuman primates II*. Berlin (Germany): Springer-Verlag.
4. Chesney CF, Allen JR. 1972. Spontaneous osteogenic sarcoma in a stump tail (*Macaca arctoides*) monkey. *J Natl Cancer Inst* 49:139–146.
5. Cianciolo RE, Butler SD, Eggers JS, Dick EJ, Leland MM, de la Garza M, Brasky KM, Cummins LB, Hubbard GB. 2007. Spontaneous neoplasia in the baboon (*Papio* spp.). *J Med Primatol* 36:61–79.
6. Deinhardt JB, Devine J, Passovoy M, Pohlman R, Deinhardt F. 1967. Marmosets as laboratory animals. I. Care of marmosets in

- the laboratory, pathology, and outline of statistical evaluation of data. *Lab Anim Care* 17:11–29.
7. **Emedicine Specialties**. [Internet]. 2009. Dermatology: diseases of the oral mucosa. Oral fibromas and fibromatoses. [Cited 22 Mar 2010]. Available at: <http://emedicine.medscape.com/article/1080948-overview>.
 8. **Eversole LR, Merrell PW, Strub D**. 1985. Radiographic characteristics of central ossifying fibroma. *Oral Surg Oral Med Oral Pathol* 59:522–527.
 9. **Granados R, Carrillo R, Nájera L, García-Villanueva M, Patrón M**. 2006. Psammomatoid ossifying fibromas: immunohistochemical analysis and differential diagnosis with psammomatous meningiomas of craniofacial bones. *Oral Surg Oral Med Oral Pathol Oral Radiol Endod* 101:614–619.
 10. **Gregson RL, Offer JM**. 1981. Metastasizing chondrosarcoma in laboratory rats. *J Comp Pathol* 91:409–413.
 11. **Hasegawa T, Seki K, Yang P, Hirose T, Hizawa K, Wada T, Wakabayashi J**. 1995. Differentiation and proliferative activity in benign and malignant cartilage tumors of bone. *Hum Pathol* 26:838–845.
 12. **Hatano H, Ogoe A, Hotta T, Otsuka H, Takahashi HE**. 1997. Periosteal chondrosarcoma invading the medullary cavity. *Skeletal Radiol* 26:375–378.
 13. **Hoang MP, Suarez PA, Donner LR, Ro JY, Ordñez NG, Ayala AG, Czerniak B**. 2000. Mesenchymal chondrosarcoma: a small-cell neoplasm with polyphenotypic differentiation. *Int J Surg Pathol* 8:291–301.
 14. **Kaspereit J, Friderichs-Gromoll S, Buse E, Habermann G**. 2007. Spontaneous neoplasms observed in cynomolgus monkeys (*Macaca fascicularis*) during a 15-year period. *Exp Toxicol Pathol* 59:163–169.
 15. **Knight JA, Wadsworth PF**. 1981. Osteosarcoma of the tibia in a squirrel monkey (*Saimiri sciureus*). *Vet Rec* 109:385–386.
 16. **Kumar SKS, Ram S, Jorgensen MG, Shuler CF, Sedghizadeh PP**. 2006. Multicentric peripheral ossifying fibroma. *J Oral Sci* 48:239–243.
 17. **Liu SK, Dorfman HD, Hurbitz AL, Patnaik AK**. 1977. Primary and secondary bone tumors in the dog. *J Small Anim Pract* 18:313–326.
 18. **McCauley CT, Campbell GA, Cummings CA, Drost WMT**. 2000. Ossifying fibroma in a llama. *J Vet Diagn Invest* 12:473–476.
 19. **Miller MA, Towle HAM, Heng HG, Greenberg CB, Pool RR**. 2008. Mandibular ossifying fibroma in a dog. *Vet Pathol* 45:203–206.
 20. **Morse CC, Saik JE, Richardson DW, Fetter AW**. 1988. Equine juvenile mandibular ossifying fibroma. *Vet Pathol* 25:415–421.
 21. **Murphey MD, Walker EA, Wilson AJ, Kransdorf MJ, Temple HT, Gannon FH**. 2003. From the archives of the AFIP. Imaging of primary chondrosarcoma: radiologic–pathologic correlation. *Radiographics* 23:1245–1278.
 22. **Nietzschman HR, Mena JC, Valle DE, Ramirez JA, Kaakaji Y, Sandoz JC, Chlapin DB, McCarthy KE**. 1998. Musculoskeletal case of the day. *Am J Roentgenol* 171:861–869.
 23. **Pritzker KPH, Kessler MJ**. 1998. Diseases of the musculoskeletal system, p 416–459. In: Bennett BT, Abee CR, Henrickson R, editors. *Nonhuman primates in biomedical research: diseases*. San Diego (CA): Academic Press.
 24. **Rankow RM**. 1947. Bilateral fibroosteoma of the maxilla in a monkey. *J Dent Res* 26:333–336.
 25. **Ratcliffe HL**. 1930. Tumors in captive primates with a description of a giant-cell tumor in a chacma baboon, *Papio porcarius*. *J Cancer Res* 14:453–460.
 26. **Reed C, Garman RH**. 1977. Osteosarcoma in a squirrel monkey. *J Am Vet Med Assoc* 171:976–979.
 27. **Rogers AB, Gould DH**. 1998. Ossifying fibroma in a sheep. *Small Rumin Res* 28:193–197.
 28. **Russell SW, Jenson FC, Vanderlip JE, Alexander NL**. 1979. Osteosarcoma of the mandible of a baboon (*Papio papio*): Morphological and virological (oncornavirus) studies, with a review of neoplasms previously described in baboons. *J Comp Pathol* 89:349–360.
 29. **Sakamoto A, Oda Y, Oshiro Y, Tamiya S, Iwamoto Y, Tsuneyoshi M**. 2001. Immunoeexpression of neurofibromin, S-100 protein, and Leu-7 and mutation analysis of the NF gene at codon 1423 in osteofibrous dysplasia. *Hum Pathol* 32:1245–1251.
 30. **Thompson K**. 2007. Diseases of bones, p 2–129. In: Maxie MG, editor. *Jubb, Kennedy, and Palmer's pathology of domestic animals*, vol 1. Edinburgh (Scotland): Elsevier Saunders.
 31. **Turrel JM, Pool PR**. 1982. Primary bone tumors in the cat: a retrospective study of 15 cats and a literature review. *Vet Radiol* 23:152–166.
 32. **Whitten KA, Popielarczyk MM, Belote DA, McLeod GC, Mense MG**. 2006. Ossifying fibroma in a miniature rex rabbit (*Oryctolagus cuniculus*). *Vet Pathol* 43:62–64.
 33. **Worawongvasu R, Songkarn K**. 2010. Fibro-osseous lesions of the jaws: an analysis of 122 cases in Thailand. *J Oral Pathol Med* 39:703–708.
 34. **Yasuda H, Taniguchi Y, Shigeta Y**. 1990. Peripheral neuropathy associated with osteosarcoma in a Japanese monkey. *Jikken Dobutsu* 39:285–289.
 35. **Zupi A, Ruggiero AM, Insabato L, Senghore N, Califano L**. 2000. Aggressive cemento-ossifying fibroma of the jaws. *Oral Oncol* 36:129–133.